IET Intelligent Transport Systems

WILEY

IET The Institution of Engineering and Technology

ORIGINAL RESEARCH OPEN ACCESS

Multi-Objective Multi-Step Adaptive Traffic Control (MOMSATC): Prioritising Pedestrians for a Safe and Sustainable Transport Development

Lok Sang Chan | Xiaocai Zhang | Neema Nassir | Majid Sarvi

Faculty of Engineering and Information Technology, The University of Melbourne, Victoria, Australia

Correspondence: Xiaocai Zhang (xiaocai.zhang@unimelb.edu.au)

Received: 27 July 2025 | **Revised:** 12 December 2025 | **Accepted:** 5 January 2026

ABSTRACT

This paper introduces MOMSATC, an innovative multi-objective, multi-step adaptive traffic signal control framework grounded in the principles of model predictive control. MOMSATC is specifically designed to address complex, high-dimensional optimisation challenges, including the mitigation of pedestrian and vehicle safety risks alongside delay management. The framework first establishes a hybrid safety evaluation model to comprehensively assess conflicts involving vulnerable road users, providing input to a multi-task learning model that predicts safety and delay outcomes. Safety risks are translated into a quantifiable monetary cost equivalent using a willingness-to-pay approach that considers long-term health and socio-economic impacts. The overarching aim of MOMSATC is to support an interpretable decision process that can represent objective priorities in a transparent manner. By integrating predictive modelling with a structured optimisation procedure, the framework allows pedestrian safety to be prioritised while maintaining a balance between vehicle safety and overall operational efficiency. A case study demonstrates the efficacy of MOMSATC, achieving significant reductions in safety risks for both pedestrians and vehicles, with moderate trade-offs in delay, underscoring its potential to achieve a safety-orientated urban transport system.

1 | Introduction

With the climate crisis driving a need for sustainable transport solutions, policymakers and researchers are increasingly focused on reducing transport emissions. Australia, for example, has set a goal of net-zero emissions by 2050 [1]. Key to achieving this goal is establishing mode shift targets that encourage walking, cycling and public transport use. This emphasises the importance of accessible urban development that transitions away from car-centric models towards more environmentally friendly modes [2]. Such initiatives will play a crucial role in mitigating transport's environmental impact.

Walkability, a measure of how conducive an area is to walking [3], is influenced by factors like destination proximity, population density and land-use diversity. Importantly, micro-scale factors like road user safety also contribute to walkability [4]. Unsafe pedestrian environments characterised by high traffic volumes, vehicle-orientated designs and inadequate crosswalks deter active transport choices.

Prioritising the safety of pedestrians often refers as vulnerable road users (VRUs), is essential to encourage active transport modes and enhance public health. The [5] estimated 1.19 million road traffic fatalities in 2021, with 50% being VRU (including pedestrians, cyclists and riders of two- and three-wheelers). In Australia, road crash deaths reached 1194 in 2022, marking a 5.8% increase from 2021 [6]. VRU accounted for 37.1% of these fatalities, with pedestrian deaths increasing by a concerning 23.3%. Intersections are hotspots for vehicle-pedestrian collisions due to their complex traffic movements.

Pedestrian crash data from Victoria, Australia (2010–2019) highlights the severity of this issue. Intersections accounted for a significant proportion of fatal (57.3%), major (50%) and minor (44.1%) injuries [7]. Further, most fatal (67.9%), major (72.8%) and minor (69%) injuries occurred while crossing the roadway, emphasising the importance of safe crosswalk provisions.

The promotion of active transport modes necessitates a shift in urban transport design. Ensuring safe operations is fundamental to reducing crash likelihood and severity, and effective outcomes depend on jointly addressing safety and efficiency. Accordingly, this paper examines pedestrian safety at intersections from a traffic operations perspective, laying the groundwork for future multi-objective traffic signal optimisation. Although recent studies have applied data driven and learning based approaches to multi objective signal control, most rely on single reward formulations that embed safety-efficiency trade offs implicitly. Existing work also emphasises surrogate safety indicators without incorporating injury severity or economic consequence, and few approaches offer an interpretable mechanism for explicitly prioritising VRU safety. These gaps motivate the development of the framework proposed in this study. The contributions of this study are as follows:

1. A hybrid safety evaluation framework is developed, which comprehensively considers both the likelihood and severity of vehicle–vehicle and pedestrian–vehicle conflicts. The safety risk is translated into a quantifiable monetary cost equivalent using the willingness-to-pay approach, taking into account the long-term impact on health and socio-economic factors.
2. A multi-task learning (MTL) model is developed, capable of processing time-series traffic and signal data to predict safety and delay outcomes across various operational settings. The use of the MTL model follows the predictive principles of model predictive control (MPC), forecasting future system states to facilitate informed decision-making for optimising traffic signal control.
3. A novel multi-objective, multi-step (MOMS) optimisation framework for adaptive traffic signal control strategies is proposed. This interpretable control policy enables explicit and transparent prioritisation of various objectives, such as pedestrian and vehicle safety.
4. Case studies demonstrate the potential for enhancing pedestrian-friendly intersections through traffic operations optimisation. Multiple two-phase traffic signal programs designed to prioritise pedestrian safety are identified and evaluated in the case study.

This paper is organised as follows: Section 2 provides a comprehensive review of existing literature on safety evaluations for VRUs, as well as pedestrian-friendly crossing design and operations. Section 3 details the proposed hybrid safety evaluation framework, focusing on the comprehensive workflow of the machine learning-based intervention policy: Multi-objectives multi-steps adaptive traffic control (MOMSATC). In Section 4, the application of MOMSATC is demonstrated, and its performance is evaluated through a case study. This section discusses the achieved results and highlights potential avenues for future research. Finally, Section 5 concludes the paper by summarising the key findings and contributions.

2 | Literature Review

The alarming rise in pedestrian fatalities demands urgent action to improve safety at intersections. This review examines studies on safety evaluation methods, considering both crash risks and injury severity. Additionally, we explore research on operational approaches to enhancing pedestrian safety.

2.1 | Vulnerable Road Users Crash Risk Modelling

A significant amount of research has focused on evaluating pedestrian-vehicle conflicts, utilising various indicators and advanced data sources. Ref. [8] employed unmanned aerial vehicles to analyse conflicts at an urban intersection. Using surrogate safety measures (SSMs) such as post-encroachment time (PET) and relative time to collision (RTTC), the study revealed high pedestrian risk both within and outside crosswalks, as well as risky right-turn manoeuvrers in a left-hand driving environment.

Ref. [9] developed a method using roadside LiDAR sensors to generate high-resolution traffic trajectories. Analysing vehicle speed-distance profiles (SDP) allows for the effective identification of near-crash events. The authors suggest this model is adaptable to different sites through threshold adjustments and has potential future applications for other conflict types, such as vehicle-bicycle interactions.

Building on this, [10] presented an improved method for identifying pedestrian-vehicle near-crashes, leveraging roadside LiDAR sensors as well. Their approach incorporated data processing algorithms for lane identification, object clustering, and tracking to extract individual road user trajectories. Employing PET, the proportion of stopping distance (PSD), and crash potential index, they offer a practical solution for site-specific conflict identification, complementing naturalistic driving study data for safety evaluation.

Meanwhile, [11] proposed a long short-term memory (LSTM) neural network model for forecasting pedestrian conflicts 2 s in advance, using PET and leveraging computer vision for detection and tracking. They claim the model is transferable to new sites with modest additional data (30%), suggesting cross-site adaptability.

Subsequently, [12] utilised CCTV footage, PET and TTC, and automated traffic signal performance measures systems to identify pedestrian conflicts and estimate exposure. Their extreme gradient boosting (XGBoost) model demonstrates the potential for proactive traffic management by predicting conflicts one cycle ahead, especially within emerging connected vehicle (CV) environments.

Similarly, [13] investigated the use of SSMs, including spatial and temporal gaps, RTTC, and PET, to assess pedestrian safety at midblock signalised crossings, extracting trajectory data from roadside cameras via computer vision. Finally, [14] and [15]

explored pedestrian crash risk assessment using extreme value theory. Ref. [14] modelled risk at the arterial corridor level using autonomous vehicle sensor data, while [15] proposed a hybrid model using AI-processed camera data to identify extreme conflicts. Both demonstrate the potential of these approaches and CV data in pedestrian safety analysis.

While these studies provide valuable methods for detecting or predicting pedestrian conflicts, most rely solely on SSMs and do not integrate injury severity or economic consequence. These limitations motivate the hybrid likelihood—severity safety evaluation developed in this study.

2.2 | Vulnerable Road Users Injury Severity

Understanding the relationship between impact speed and injury severity is crucial for developing effective safety interventions for VRU. In vehicle-pedestrian collisions, VRU lacks the protection of energy-absorbing vehicle structures, making injury severity directly correlated with impact speed [16]. Early 21st-century research consistently demonstrated this association, although findings varied slightly due to factors like data source, demographics and vehicle technology (Scully et al., 2007, as cited in Archer et al., [16]). Ref. [17] extended this analysis by predicting both fatality risk and the likelihood of serious injuries as defined by the maximum abbreviated injury scale (MAIS).

Recently, [18] sought to define precise injury risk curves, establishing mathematical relationships between closing speed and injury outcomes for various road users. Using weighted binary logistic regression, they modelled injury probabilities as a function of closing speed and age, considering three injury severity levels aligned with the MAIS 2015 revision: at-least-moderate (MAIS2+), at-least-serious (MAIS3+) and fatal injuries. For instance, a vehicle-pedestrian encounter at 25 km/h corresponds to a 10% risk of a pedestrian sustaining a serious injury.

Beyond statistical modelling, machine learning (ML) offers insights into vehicle-pedestrian injury severity. Ref. [19] used a support vector machine (SVM) to classify severity levels and analyse the importance of variables such as speed, gap time, TTC and PET. Their analysis revealed varying contributions of these indicators to severity across different conflict types, prompting the authors to recommend tailored indicators for specific scenarios.

Ref. [20] employed a deep learning framework for VRU injury severity prediction. Their methodology involved a combination of techniques: a CatBoost model for feature selection, clustering approaches for data classification, and prediction using a stacked sparse autoencoder. Meanwhile, several studies proposed hybrid approaches combining various techniques with random parameters discrete outcome analysis. Examples include [21] use of Bayesian networks, [22] employment of XGBoost and [23] use of random forest. Additionally, the SHapley Additive exPlanations method [24] aided in interpreting feature importance within models such as CatBoost, XGBoost and random forest.

2.3 | Safe Pedestrian Crossing Design and Operations

Traffic engineers continuously strive to optimise intersection safety and efficiency. A significant body of research has explored techniques for segregating conflicting traffic flows, such as continuous flow intersections (CFIs) [25–27], tandem intersections [28, 29] and turn movement separated intersections [30]. While these methods enhance traffic flow, they may introduce complex signage and signal displays that can be confusing for unfamiliar drivers. Furthermore, the pre-sorting phase often takes place within a mid-block location, requiring additional space to accommodate separated vehicles. This can potentially lead to temporary 'against-flow' situations. In densely populated areas, securing this extra space can be a significant challenge.

With the increased presence of pedestrians, ensuring their crossing safety while maximising operational efficiency becomes a critical issue. Common approaches for managing conflicts between pedestrians and vehicles involve spatial and temporal separation. Grade-separated pedestrian systems (GSPS), encompassing underground pedestrian systems and skywalk networks (or a combination of both), exemplify complete spatial separation from street-level vehicle traffic [31]. Ref. [32] conducted a systematic review of GSPS development, concluding that these systems offer potential economic benefits, particularly in densely populated urban areas, by providing protection from weather and vehicle traffic. However, concerns exist regarding potential declines in the value of street-level spaces and the infrastructure costs associated with connecting pedestrians to the GSPS network.

To promote pedestrian safety at street-level intersections, various design solutions have been explored. Ref. [33] focused on pedestrian crossing facilities within CFIs, introducing an interlaced crossing pattern, sub-intersections, and exclusive pedestrian phasing to enhance safety and efficiency. Beyond CFIs, studies have assessed additional safety measures. Ref. [34] highlighted the importance of marked crosswalks, speed cushions and visibility enhancements, especially for vulnerable pedestrians. For wide intersections, a recurring theme is the use of refuge islands to provide safety for pedestrians. Ref. [35] stressed their necessity, while [36] incorporated them into a two-stage CFI crossing pattern. Ref. [37] extended this research to symmetric intersections, finding refuge islands more effective than diagonal phasing alone for pedestrian protection, with minimal impact on traffic efficiency.

Although the implementation of pedestrian crossing facilities enhances safety, their integration into existing intersections can be limited by site geometry, urban density, and infrastructure costs. Consequently, operational modifications offer a potentially low-cost alternative to improve pedestrian safety with minimal changes to existing infrastructure.

Typical operational considerations centre on providing exclusive pedestrian phases to minimise conflicts between pedestrians and vehicles [38–40]. Research exploring pedestrian signal phasing dates back to the late 20th century, with [41] examining various schemes including the exclusive, concurrent, early or late release of pedestrians. This study recommended phasing

strategies tailored to specific pedestrian volumes and vehicle-turning movements.

Similarly, [42] and [43] conducted comparative studies of concurrent, exclusive phasing and unsignalised intersections, utilising pedestrian collision data from the United States and Israel, respectively. Both studies concluded that exclusive pedestrian phases were associated with a reduction in pedestrian collisions, particularly in areas with moderate pedestrian volumes.

Subsequent research by [44] analysed conflict data from various Swedish intersections, suggesting that the effectiveness of exclusive phasing on pedestrian safety is influenced by the number of jaywalkers. Similarly, [45] and [46] compared safety performance before and after the implementation of exclusive signals in California and Alberta, respectively. Both studies noted a significant decrease in conflict frequency, yet observed a corresponding increase in pedestrian violations.

Ref. [47] investigated safety effects through interaction severity, revealing a trade-off: intersections with concurrent phasing typically experience fewer crashes compared to exclusive phasing, but those crashes tend to be more severe. Conversely, [48] explored pedestrian compliance effects of exclusive phasing in Connecticut, United States. Their findings suggest that pedestrians are not more likely to jaywalk in exclusive phasing crosswalks, supporting the expected safety benefits of this approach.

Ref. [49] explored a potential solution based on leading pedestrian intervals (LPI). This early start technique aims to reduce the 'surprise' of pedestrian presence for turning vehicles. Their results indicated that LPI significantly reduced pedestrian crash risk by 42% without negatively impacting rear-end conflicts among turning vehicles.

2.4 | Multi-Objective ATSC

In addition to traditional control strategies and signal timing designs, safety-orientated adaptive traffic signal control (ATSC) is gaining prominence in proactive traffic management. Earlier ATSC optimisation methods focused predominantly on transport efficiency, yet the increasing shift toward multimodal transport has raised concerns about road user safety. Consequently, a growing body of research aims to incorporate safety considerations into traffic signal control [50–53].

Ref. [52] proposed a multi-objective model that integrates traffic mobility, SSMs and environmental factors. Field experiments demonstrated this model's superiority over conventional signal timing methods, showcasing the practical potential of evolutionary algorithms for optimisation in traffic signal control. Similarly, [51] optimised signal settings and lane assignments using the cell mapping method combined with microscopic simulation, achieving improvements across safety, mobility, and energy consumption.

Building on this, [53] introduced a multi-objective deep reinforcement learning (DRL) framework that jointly optimises efficiency and safety, supported by a crash prediction model. More recently, [50] developed the SafeLight framework, which embeds an explicit safety module into DRL-based control to mitigate unsafe left-turn scenarios, showing that integrating safety filtering into DRL can reduce collision risks without degrading efficiency.

These studies illustrate a gradual evolution from efficiency-focused optimisation toward safety-aware adaptive control. At the same time, modern ATSC systems increasingly rely on SSMs such as TTC and PET to anticipate near-misses. However, most work remains vehicle-centric, with limited emphasis on VRUs and limited integration of injury severity or economic consequence modelling.

Recent research has pushed further toward multi-objective optimisation for mixed pedestrian–vehicle environments. Ref. [54] introduced PV-TSC, a DRL framework designed to jointly model pedestrian and vehicle flows, though its optimisation remains largely throughput-focused. Ref. [55] advanced this by proposing the IVPL system, which explicitly targets pedestrian-vehicle conflict zones, placing pedestrian safety at the centre of the optimisation. Ref. [56] broadened multi-objective DRL to include safety, efficiency, and decarbonisation, yet did not fully address conflicting objectives or multi-intersection coordination. Ref. [57] contributed a complementary perspective by optimising pedestrian shuttle services within autonomous intersection management, relevant to future CAV-integrated networks.

More recently, [58] proposed TS-PVL, a two-stage DRL structure that learns separate policies for pedestrians and vehicles, offering improved flexibility in mixed-autonomy environments. Likewise, [59] developed a DRL controller using connected-vehicle data to enhance pedestrian safety while preserving vehicle efficiency, though its assumptions regarding data availability limit generalisability.

Recent advances in adaptive traffic signal control increasingly draw on data driven and learning based methods, with DRL techniques widely explored for multi objective signal control because of their capacity to model complex interactions within traffic systems. However, these approaches typically employ end to end control policies in which safety, efficiency and other objectives are combined through a single reward function. The resulting trade offs are therefore encoded implicitly within the weighting scheme, limiting the transparency of how safety is prioritised and making the rationale for action selection difficult to interpret. This creates a black box decision process in which the influence of each objective cannot be directly verified. A conceptual distinction is therefore needed between prediction components, which naturally involve trainable parameters, and the downstream decision mechanism, which should offer explicit and controllable prioritisation of objectives, particularly for VRU. Current DRL studies rarely articulate this separation, highlighting an opportunity for frameworks that retain the predictive strength of data driven models while providing a clear, interpretable, and prioritised multi objective decision structure.

3 | Methodology

3.1 | Pedestrian Safety Risk Evaluation

The pedestrian safety evaluation framework presented in this study extends the vehicle–vehicle conflicts evaluation framework

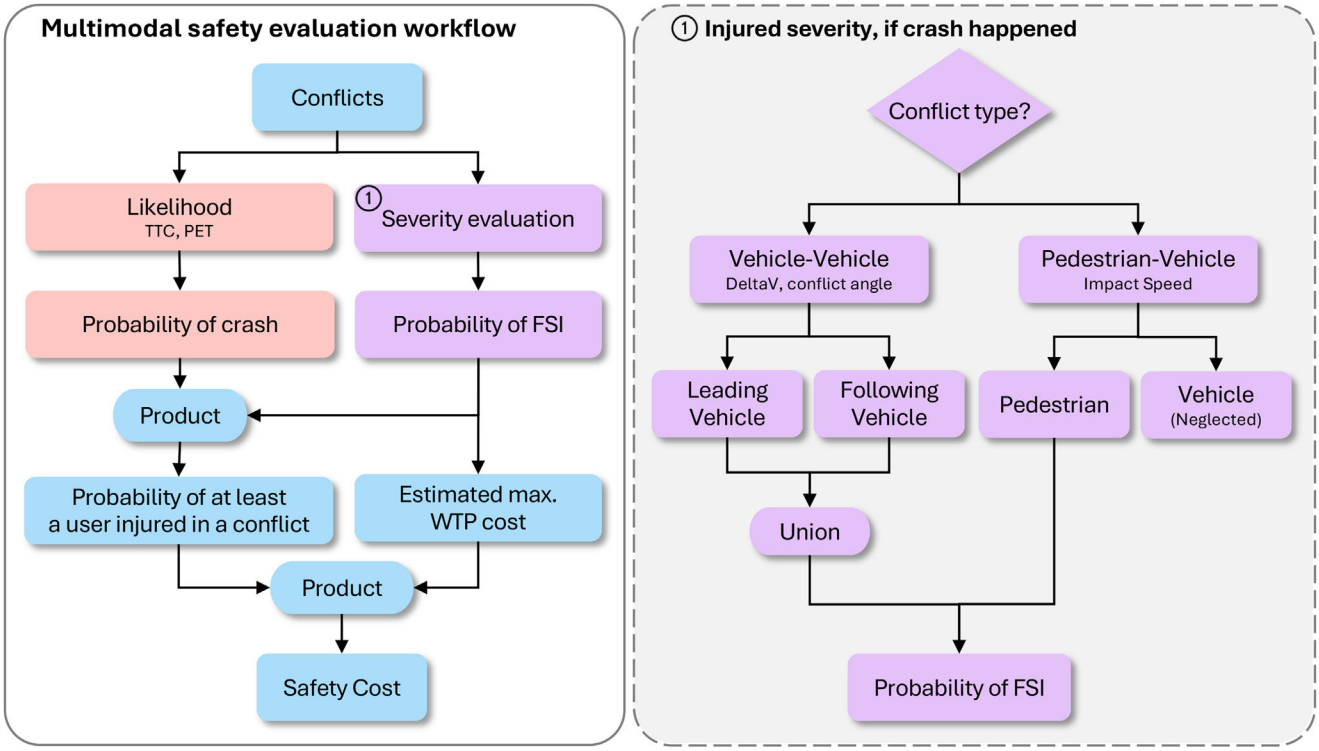

FIGURE 1 | Proposed safety evaluation framework.

outlined in [60]. The original framework provided a cost-based safety evaluation approach that considers the probability and severity of near-miss events, converting safety risk to economic and human costs. This revised framework (Figure 1) is designed to facilitate a comprehensive multi-objective signal optimisation model that balances objectives of safety and efficiency.

A substantial body of research has investigated the influence of various risk factors, including impact speed, gap time and demographic characteristics, on pedestrian injury severity in vehicle-to-pedestrian collisions (detailed in Section 2.2). This study adopts the logistic regression model developed by [18] to examine this relationship. It is important to note that [18] define injury risk using the vehicle–pedestrian closing speed. In the context of a collision, the closing speed at the moment of impact corresponds directly to the impact speed. The two terms are therefore interchangeable in this study. Assuming a pedestrian–vehicle crash has occurred, this model calculates the probability of fatal and severe injuries (FSI), defined as those with a maximum abbreviated injury scale score of 3 or higher (MAIS3+), that is,

$$\Pr(\mathrm{FSI}_{\mathrm{ped}}) = \frac{1}{1+e^{-t}}, \tag{1}$$

where t depends on both the impact speed (υ) and the pedestrian's age (α), that is,

$$t = -6.190 + 0.078(\upsilon) + 0.038(\alpha). \tag{2}$$

Figure 2 presents the logistic injury–risk curves for three representative ages within the model's valid range of 15–79 years. These ages, 15, 46 and 79, respectively reflect the lower bound,

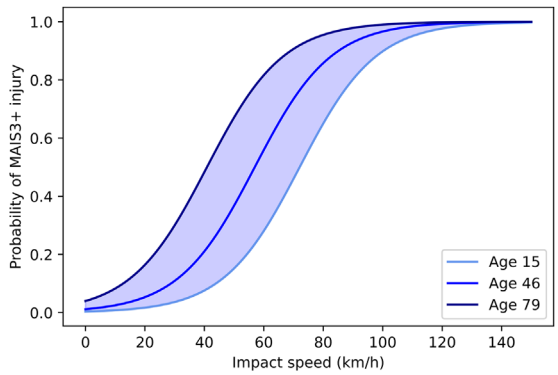

FIGURE 2 | Illustration of consequence of crash versus impact speed.

the median age of injured pedestrians reported by [61], and the upper bound of the applicable age interval. The use of discrete curves is intended to illustrate how injury probability shifts with age while highlighting impact speed as the dominant factor. For the subsequent analysis, the median age of 46 is adopted to isolate the effect of speed and avoid introducing age as an additional modelling variable. It is also assumed that vehicle occupants experience mitigated injury severity compared to pedestrians due to the lesser direct exposure to impact forces [16].

Turning to the likelihood of a crash, extensive research has explored crash risk modelling using various conflict indicators (see Section 2.1). Studies have also employed conflict indicators and analytic models, such as extreme value theory, to estimate crash potential [62–67]. Following [63], this study adopts a TTC–based exponential decay model, where TTC represents the time

TABLE 1 | Inclusive willingness-to-pay per accident.

Severity level	Urban	Rural	Average
Fatality	$7,808,768	$9,242,523	$8,586,767
Serious injury	$507,553	$700,151	$574,265
Moderate injury side	$85,296	$112,608	$97,512
Minor injury side	$78,389	$103,484	$89,314
Property damage only	$10,338	$10,338	$10,338

Source: Reprinted from Transport for NSW Economic Parameter Values, Transport for New South Wales (TfNSW), 2022, p. 31.

TABLE 2 | Definition of preset signal program.

Action	Sequence	Action	Sequence	Action	Sequence
S_1	$E_1 \rightarrow E_4$	S_7	$E_3 \rightarrow E_5$	S_{13}	$E_5 \rightarrow E_4$
S_2	$E_1 \rightarrow E_6$	S_8	$E_3 \rightarrow E_6$	S_{14}	$E_5 \rightarrow E_6$
S_3	$E_4 \rightarrow E_1$	S_9	$E_5 \rightarrow E_3$	S_{15}	$E_6 \rightarrow E_4$
S_4	$E_6 \rightarrow E_1$	S_{10}	$E_6 \rightarrow E_3$	S_{16}	$E_6 \rightarrow E_5$
S_5	$E_2 \rightarrow E_6$	S_{11}	$E_4 \rightarrow E_5$	S_{17}	$E_6 \rightarrow E_6$
S_6	$E_6 \rightarrow E_2$	S_{12}	$E_4 \rightarrow E_6$		

Abbreviations: S_i = Signal program i, E_j = Elementary phase j.

remaining until impact if both road users continue with their current speed and trajectory. The model is expressed as,

$$\Pr(C) = a + b \times e^{\frac{-\mathrm{TTC}}{c}}. \tag{3}$$

For a probability range between 0 and 1, the coefficients a and b are set to 0 and 1. The decay parameter c controls how quickly the crash likelihood diminishes as TTC increases. Although several factors may influence this decay rate, driver reaction time offers a practical behavioural guide for selecting an appropriate value. In this study, a representative reaction time of approximately 1.5 s is used to inform the choice of c, leading to a decay rate that yields very low crash likelihood once TTC exceeds this reaction time threshold. Substituting the selected value of c gives,

$$\Pr(C) = e^{\frac{-\mathrm{TTC}}{0.5}}. \tag{4}$$

Consequently, the probability of a crash resulting in FSI for a pedestrian can be calculated as the product of the consequence (impact and injury severity) and the likelihood of the crash itself, that is,

$$\Pr(\mathrm{FSI}_{\mathrm{ped}} \wedge C) = \Pr(\mathrm{FSI}_{\mathrm{Ped}}) \times \Pr(C). \tag{5}$$

To ensure cross-objective comparability in a future optimisation model encompassing safety, delays and emissions, it is necessary to translate safety risk into a quantifiable monetary cost equivalent. The literature offers several established approaches for quantifying crash events, notably the human capital (HC) and value of risk reduction (VRR) methods [68–71].

The HC method prioritises tangible costs associated with crashes, such as hospitalisation expenditures, income loss, and property damage. Conversely, the VRR approach emphasises individuals' willingness-to-pay (WTP) to mitigate crashes resulting in fatalities or injuries. Studies by [69] and [71] provide methodological frameworks for estimating WTP. Significantly, the latter study aligns with the 'inclusive WTP' approach mandated by the Australian Government Department of Infrastructure, Transport, Cities, and Regional Development and adopted by the Australian Transport Assessment and Planning Guidelines. Consequently, this study leverages the inclusive WTP values provided by Transport for New South Wales (Table 1).

Given our focus on urban intersections, a two-step procedure can be employed to calculate the safety cost of a near-miss event using urban inclusive WTP values. Firstly, the potential maximum cost is established by aligning the crash consequence to the corresponding severity level. Subsequently, this cost is multiplied by the probability of a fatal crash to yield an estimate of the overall safety cost associated with the near-miss event. This two-step consequence—likelihood procedure is consistent with the framework established in our previous study [60], where the detailed derivation, severity mapping and worked examples are presented. The present study focuses on an Australian intersection and reflects the corresponding signal design practice and parameter values. Applying the framework elsewhere would require calibration using regional safety, behaviour and valuation data.

3.2 | Pedestrian Crossing Phasing and Modelling

This study investigates a four-lane, four-approach intersection located within the Australian Integrated Multimodal EcoSystems (AIMES) testbed in Carlton, Melbourne, Australia [55]. Each approach features a dedicated right-turn lane, with left turns permitted only from the leftmost lane.

The intersection utilises a conceptual adaptive two-stage (g), two-phase traffic signal control system. The North–South (NS) and East–West (EW) stages, each comprised of two out of the six elementary phases detailed in Figure 3, operate sequentially. These elementary phases are designed with varying priority levels. Elementary phases E_1 and E_2 prioritise turning movements, while E_3 provides exclusive green time for pedestrians. Phases E_4, E_5 and E_6 accommodate different pairs of conflicting traffic movements.

Seventeen signal programs were chosen from a pool of 30 possible permutations (refer to Table 2). These programs were selected to ensure that every traffic flow had at least one designated exit opportunity within a stage. In addition to the selection of signal programs, variations in phase durations were also considered. The reported phase durations are inclusive of transition times, encompassing both vehicle amber and clearance red times or flashing red for pedestrians. This implies that the elementary phase logic will autonomously adjust to satisfy minimum time requirements based on its position within the stage and the associated road user types. For phases accommodating both vehicles and pedestrians, the flashing pedestrian signal is guaranteed to terminate before the vehicle signal transitions to amber. Therefore, minimum duration requirements are established for each

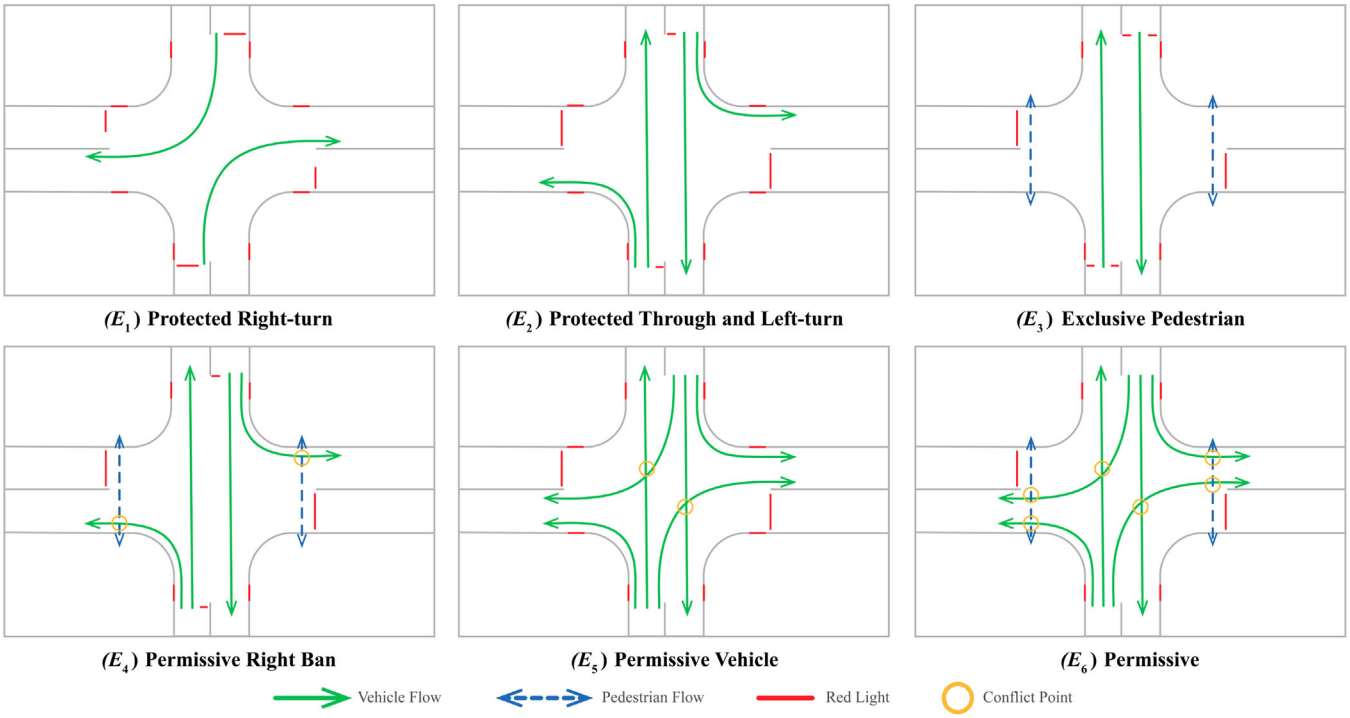

FIGURE 3 | Elementary phases.

phase within their corresponding programs. Detailed information regarding all signal settings is presented in Table 3.

3.3 | Microsimulation Settings

Traffic simulation offers a valuable methodology for modelling safety performance. This approach presents several advantages, including the ability to efficiently collect data and proactively evaluate conceptual models. Continued research in this domain holds promise for further improvements in the accuracy and applicability of simulation-based safety assessment models. This study utilises Vissim, a microsimulation software developed by the [72], to model the four-lane, four-approach intersection. In conjunction with microsimulation, the surrogate safety assessment model (SSAM) software package, published by the [73] of the United States, is employed to extract conflict profiles from the simulated vehicle trajectories. Several studies have found utilising SSAM for conflict identification in simulated environments [74–77].

SSAM identifies conflicts within trajectories based on two key conflict indicators: TTC and PET. TTC represents the time required for two vehicles to collide if they maintain their current speeds and paths [78]. PET, on the other hand, refers to the time difference between a vehicle exiting a potential collision zone and the arrival of another vehicle [79]. Thresholds for these indicators vary across studies, with suggestions ranging from 1.5 to 5 s for TTC and 1 to 4 s for PET [80, 81]. To ensure comprehensive conflict capture, considering that the proposed framework will involve further conflict analysis, this study adopts thresholds of 5 s for TTC and 4 s for PET. Additional details regarding the simulation settings have been provided in Table 3.

3.4 | MOMSATC

The workflow of the proposed multi-objective, multi-step adaptive traffic control (MOMSATC) is illustrated in Figure 4, which consists of four major components: data preprocessing, action spaces, prediction model, and optimisation module. Data preprocessing involves procedures to prepare data for machine learning and prediction. Initially, various traffic volume scenarios are simulated using a microsimulation model, with random signal actions assigned for each cycle, generating sequences of operations. The simulation performance is collected, recording signal operations, trajectories and detected conflicts. This data is then processed to train the multi-task prediction model. The data is divided into observation-action pairs based on time. Observations consist of time-series data collected 5 min before the operation decision is made, while actions comprise the chosen action for the next cycle and its corresponding performance metrics, including safety costs and delays. MOMSATC leverages the predictive principle of MPC for traffic signal control [82]. The prediction model evaluates all feasible actions and forecasts their potential outcomes. Based on these forecasts, the optimisation module selects the optimal action, which is then implemented for the subsequent control cycle.

3.4.1 | Observation Definition

Given recent advancements in traffic flow detection technologies and the availability of high-resolution data from cameras or connected vehicles, our model assumes the detection of individual vehicle and pedestrian arrivals within a 50-m radius of the interaction centre. This enables the intelligent traffic control system to utilise information within this range and convert it

TABLE 3 | Simulation environment settings.

Variable	Definition
Traffic signal parameters	
g	Active stage, g = 0 NS (North–South); g = 1 EW (East–West)
S_i	Two-phase signal programs presented in Table 2, selectable from 1 to 17
E_j	Elementary phase j presented in Figure 3, selectable from 1 to 6
D_k	Phase duration, $k = 0$ first phase; $k = 1$ second phase; [10, 40]s for vehicle only phase; [20, 40]s if pedestrian exist
$D'_{i,j,k}$	Minimum phase duration depends on phase type, signal program and corresponding position
t_{ped}	Minimum red flashing time for pedestrian crossing, 10 s
t_a	Vehicle amber time, if transition exist, 3 s
t_r	Minimum red time for clearance, if transition exist, 2 s
Simulation traffic input parameters	
λ	Approach $\lambda = 1, 2, 3, 4$ corresponds to southbound, westbound, northbound, eastbound, respectively
O_λ	Average vehicle volume per quarter hour of approach λ, [0, 300]/quarter hour
$\theta_{\lambda,i}$	Proportion of turning vehicle i, i =1 right turn; $i = 2$ left turn
Q_λ	Average pedestrian volume per quarter hour of approach λ, [0, 120]/quarter hour
Evaluation parameters	
η	Conflict type, η = veh, ped, tot corresponds to vehicle–vehicle, pedestrian–vehicle, total, respectively
TTC_{th}	TTC threshold, 5 s
pet_{th}	PET threshold, 4 s
ω	Vehicle conflict angle, °
δ_v	Maximum change in velocity recorded during the conflict, km/h
WTP_i	Willingness to pay cost i for each severity level, $i = 1$ fatal; $i = 2$ serious; i = 3 moderate; $i = 4$ minor; i = 5 P.O.D; details in Table 1
α_η	Evaluated conflict safety cost, $
$\alpha_{\eta,\text{th}}$	Conflict safety cost threshold, η = ped 100; η = veh 500, $
ρ_η	Probability of the safety performance is acceptable
β	User delay, user-second

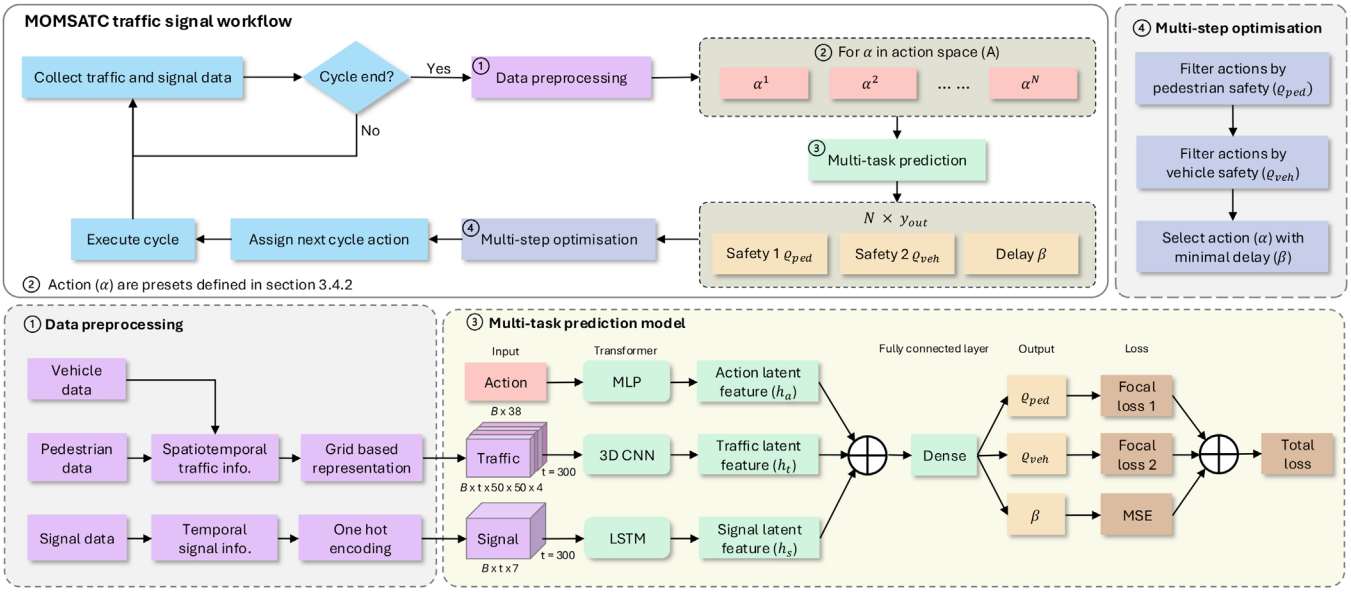

FIGURE 4 | Illustration of the MOMSATC traffic signal workflow, showing the process from feature extraction through to action selection.

FIGURE 5 | Illustration of the 50 × 50 detection zone, discretised into a grid that forms the spatial component of the traffic state matrix.

into a state matrix representation, as depicted in Figure 5. The detection zone is discretised into a 50 × 50 matrix, with each cell (i, j) representing a 2-m × 2-m block. This spatial resolution aligns with the positional accuracy typically achievable in urban vision-based and connected-vehicle sensing, and is sufficient to distinguish pedestrian presence, movement direction and proximity to conflict points at the scale relevant for intersection-level decision making. A 2-m cell also approximates the lateral footprint of a typical passenger vehicle, allowing vehicle movements to be represented without overlap while maintaining a consistent spatial structure for both pedestrians and vehicles. Subsequently, spatiotemporal occupancy and speed information are mapped into the corresponding matrices $P_{k,t}$ and $V_{k,t}$, where k = ped or veh distinguishes the traffic states for pedestrians and vehicles. An observation over the past 5 min, $1 \leqslant t \leqslant 300$, can then be represented as video-like data with four channels and 300 frames. The position and speed matrices are defined as

$$P_{k,t} = \begin{bmatrix} p_{1,1} & \cdots & p_{1,j} & \cdots & p_{1,50} \\ \vdots & \ddots & \vdots & & \vdots \\ p_{i,1} & \cdots & p_{i,j} & \cdots & p_{i,50} \\ \vdots & & \vdots & \ddots & \vdots \\ p_{50,1} & \cdots & p_{50,j} & \cdots & p_{50,50} \end{bmatrix}, \tag{6}$$

and

$$V_{k,t} = \begin{bmatrix} v_{1,1} & \cdots & v_{1,j} & \cdots & v_{1,50} \\ \vdots & \ddots & \vdots & & \vdots \\ v_{i,1} & \cdots & v_{i,j} & \cdots & v_{i,50} \\ \vdots & & \vdots & \ddots & \vdots \\ v_{50,1} & \cdots & v_{50,j} & \cdots & v_{50,50} \end{bmatrix}. \tag{7}$$

Conversely, traffic signal operations are represented by a signal state matrix. As each signal program consists of two phases (E_j), the traffic signal state is captured using a phase-type pattern. Combined with the active stage (g) and the one-hot encoded active phases, the signal state matrix is transformed into a 2D matrix. In this matrix, each row denotes a time step $(1 \leqslant t \leqslant 300)$, and the columns represent the active stage and phases, as formulated by,

$$\text{Signal}_t = \begin{bmatrix} g & E_1 & E_2 & E_3 & E_4 & E_5 & E_6 \end{bmatrix}. \tag{8}$$

The vector elements indicate the currently active stage and phases. For example, if the North–South protected right-turn phase is active, the vector becomes [0,1,0,0,0,0,0].

3.4.2 | Action Definition

In the proposed optimisation framework, the model evaluates all feasible actions to predict potential conflict risk and delays, aligning with the traffic signal settings outlined in Table 3. An action is defined as the operational decision for the next cycle, encompassing the signal program (S_i) and phase durations (D_k) of the corresponding two stages (g), equivalently,

$$\text{Action} = \begin{bmatrix} S_{i,\text{NS}} & D_{1,\text{NS}} & D_{2,\text{NS}} & S_{i,\text{EW}} & D_{1,\text{EW}} & D_{2,\text{EW}} \end{bmatrix}. \tag{9}$$

The vector above indicates the signal programs and corresponding sub-phase durations for the North–South (NS) and East–West (EW) stages. After applying one-hot encoding to the signal programs, the action becomes a 38-dimension vector.

The action space (A) is the set of actions examined by the model. It comprises various combinations of elements within the action vector. To limit the size of the action space, phase durations are discretised with a 5-s increment step, adhering to the range specified in Table 3. Consequently, the prediction model evaluates over 260,000 actions when determining the operations for the next cycle.

3.4.3 | Multi-Task Prediction Model

The prediction model considers three input data sources: observed traffic state, signal configuration, and the next-cycle action, to predict potential performance. It utilises three different representation learning models: a 3D convolutional neural network (3D CNN), an LSTM network and a multilayer perceptron (MLP), to extract useful representations, h_t, h_s and h_a, respectively. The latent features capture essential patterns and features from the raw traffic state, signal state and action inputs (Figure 4). The extracted features are subsequently combined to create the joint features (h_j), which are then used for the follow-up pattern recognition tasks. Mathematically, this process is expressed as,

$$h_t = f_{\text{3DCNN}}(x_t; \psi_t), \tag{10}$$

$$h_s = f_{\text{LSTM}}(x_s; \psi_s), \tag{11}$$

$$h_a = f_{\text{MLP}}(x_a; \psi_a), \tag{12}$$

and

$$h_j = h_t + h_s + h_a, \tag{13}$$

where x and ψ are the input and corresponding weights of each layer. A dense layer with a Sigmoid activation function is then applied to produce the prediction model's output, as indicated by

$$h_d = f_{\text{Dense}}\left(h_j; \psi_d\right), \tag{14}$$

and

$$y_{\text{out}} = \sigma_{\text{Sigmoid}}\left(h_d; \psi_{\text{sigmoid}}\right). \tag{15}$$

The proposed model predicts the potential performance of each action and selects the optimal action for the next cycle. Initially, the performance vector consists of three elements: pedestrian safety cost (α_{ped}), vehicle safety cost (α_{veh}), and road user delays (β), that is,

$$y_{\text{out}} = \begin{bmatrix} \alpha_{\text{ped}} & \alpha_{\text{veh}} & \beta \end{bmatrix}. \tag{16}$$

Each element within the vector represents the overall performance of the next cycle if the corresponding action is applied. Both pedestrian and vehicle safety costs are calculated as the cumulative sum of evaluated conflicts using the risk evaluation framework outlined in Section 3.1. Delays are measured as the total seconds each road user is trapped at the interaction, extracted from the traffic state matrices. Notably, each detected pedestrian and vehicle is treated as one road user, ensuring a more equitable weighting compared to traditional pedestrian crossings with push buttons.

However, the analysis revealed extreme values within the training data for both pedestrian and vehicle safety costs, hindering the prediction model's convergence toward a good fit. As the model primarily focuses on predicting risky situations rather than the exact cost values, the prediction of safety performance was converted from regression to imbalanced binary classification. Threshold values, $\alpha_{\eta,\text{th}}$, were established to classify safety performance as either acceptable (0) or rejected (1), where

$$\text{class}_{\text{ped}} = \begin{cases} 0, & \text{if } \alpha_{\text{ped}} < \alpha_{\text{ped,th}} \\ 1, & \text{otherwise} \end{cases} \tag{17}$$

and

$$\text{class}_{\text{veh}} = \begin{cases} 0, & \text{if } \alpha_{\text{veh}} < \alpha_{\text{veh,th}} \\ 1, & \text{otherwise} \end{cases}. \tag{18}$$

Consequently, the dependent variables are transformed into probabilities of acceptable safety performance (ρ_η), that is,

$$y_{\text{out}} = \begin{bmatrix} \rho_{\text{ped}} & \rho_{\text{veh}} & \beta \end{bmatrix}. \tag{19}$$

With the threshold values ($\alpha_{\eta,\text{th}}$) outlined in Table 3, the calculated imbalance ratios for acceptable to rejected outcomes are 13:1 and 6:1 for pedestrians and vehicles, respectively.

Furthermore, the model's parameters are optimised using the combined loss (ζ_j), formulated as the sum of the individual losses for each output, given by,

$$\zeta_j(y_{\text{out}}, y) = \zeta_{\text{focal}}(y^1_{\text{out}}, y^1) + \zeta_{\text{focal}}(y^2_{\text{out}}, y^2) + \zeta_{\text{MSE}}(y^3_{\text{out}}, y^3), \tag{20}$$

where y^i_{out} and y^i represent the predicted and ground-truth values, respectively, for the ith element in the output vector. Specifically, focal loss (ζ_{focal}) is applied to address the imbalanced classification outputs (pedestrian and vehicle safety), while mean squared error (ζ_{MSE}) is applied to the regression output (delay).

TABLE 4 | Model architecture and training configuration.

Component	Configuration
Input (traffic state)	$300 \times 50 \times 50 \times 4$ tensor
Input (signal state)	300×7 sequence
Input (action vector)	38-dimensional vector
3D CNN layers	Conv3D (32, $3 \times 3 \times 3$), MaxPool, Conv3D (64, $3 \times 3 \times 3$), MaxPool, Dense (64)
LSTM layers	LSTM (64, return seq.), LSTM (64), Dense (64)
MLP layers	Dense (64), Dense (64)
Feature fusion	Concatenation + dropout (0.3–0.6)
Output heads	Two sigmoid units (pedestrian, vehicle safety)
Optimiser	Adam ($\alpha = 0.001$)
Batch size	32
Epochs	5000 (early stopping)
Loss function	Focal loss
Normalisation	Min–max scaling

A concise summary of the model architecture and training configuration is provided in Table 4 to support reproducibility. These settings correspond to the implementation used to generate the results reported in this study. The prediction component is designed to serve as a dependable module within the wider optimisation workflow, and the intention is not to introduce architectural novelty. For this reason, widely used configurations for the 3D-CNN, LSTM, and MLP feature extractors were adopted.

Our exploratory tests indicated that the predictive behaviour is relatively insensitive to moderate variations in depth, width and sequence-processing mechanisms. Architectures such as deeper convolutional stacks or transformer-based encoders were also trialled, and these achieved similar levels of performance. This robustness suggests that the overall framework does not rely on fine-grained architectural tuning and that the performance gains observed in MOMSATC stem primarily from the integration of prediction and optimisation rather than from specific network design choices. The full training script can be made available upon reasonable request.

3.4.4 | Muti-Step Optimisation

The filter module employs a sequential filtering process to select the optimal traffic signal action from the action space (A) evaluated by the prediction model. In the initial stage, the action with the minimum probability of a pedestrian risk event ($\rho_{\text{ped, min}}$) is identified. All actions with performance within a 50% tolerance ($\tau = 0.5$) of this minimum are retained, mathematically expressed as,

$$A_1 = \{a \in A \mid \rho_{\text{ped}}(a) \leq (1+\tau) \times \rho_{\text{ped,min}}\}. \tag{21}$$

The second stage prioritises vehicle safety, identifying the action with the minimum probability of a vehicle risk event ($\rho_{\text{veh, min}}$) among the previously filtered actions (A_1) and retaining those within the 50% tolerance threshold (A_2), specifically,

$$A_2 = \{a \in A_1 \mid \rho_{\text{veh}}(a) \leq (1+\tau) \times \rho_{\text{veh,min}}\}. \tag{22}$$

Finally, the filter selects the action from the remaining set (A_2) that minimises overall user delay (β_{min}), formally represented as,

$$a_{\text{optimal}} = \underset{a \in A_2}{\text{argmin}}\ \beta(a). \tag{23}$$

This filtering approach prioritises pedestrian safety while maintaining acceptable thresholds for vehicle safety and overall user delay. The 50% tolerance is employed to ensure that the multi-task prediction model achieves a recall rate exceeding 80% on unseen test data. Recall is calculated as

$$\text{Recall} = \text{TP}/(\text{TP} + \text{FN}), \tag{24}$$

where TP and FN represent the number of true positives and false negatives, respectively. A higher recall rate indicates a lower false-negative rate, signifying the reliability of the filtered actions.

By incorporating this tolerance, the multi-step optimisation process balances safety and efficiency, ensuring the selected action not only optimises the primary objective of pedestrian safety but also maintains reasonable performance regarding other objectives. Consequently, the proposed MOMSATC workflow prioritises the safety of VRUs while seeking to optimise other objectives after mitigating risks to these users.

4 | Result and Discussion

The case study focuses on an isolated four-lane, four-approach intersection within the AIMES testbed, established by the University of Melbourne in 2016. The proposed workflow was evaluated using an isolated intersection simulation model. Figure 6 illustrates the lane configurations and the origin-destination (OD) zones defined within the simulation environment. Initially, the model generated scenarios with varying demand inputs and signal control sequences to facilitate the prediction model's learning process. The associated simulation scenario parameters are detailed in Table 3.

Simulated trajectories were exported from VISSIM at a 1-s resolution and processed through SSAM to extract conflict indicators. In total, 1000 simulation hours were generated, yielding 18,255 learning samples after preprocessing. The preprocessing procedure involved synchronising VISSIM trajectories with SSAM-derived conflict events, filtering incomplete or low-quality records, and aggregating safety and delay outcomes within the 300-s observation windows used by the prediction model. The data synthesis process follows the methodology described in [60], where the full simulation and conflict-extraction workflow is documented in detail.

The data was then split into training and testing sets, with a 7:3 ratio, respectively. Subsequently, 20% of the training data was allocated for validation to monitor validation loss during training and achieve the best-fit generalised model. Evaluation metrics, including the area under the ROC curve (AUC) for classification (pedestrian and vehicle safety) and the coefficient of determination (R^2) for regression (delays), were applied to assess the model's performance against unseen test data. A multi-task prediction model with AUC scores of 0.58 and 0.59 for pedestrian and vehicle safety risk, respectively, and an R^2 score of 0.74 for delay was selected.

While the prediction accuracy could be further improved, the present results reflect the characteristics of the simulated data, where conflict events exhibit substantial randomness and include extreme values that are difficult to learn consistently. These factors limit the achievable predictive performance with the current dataset. It is also important to note that the prediction model functions as a supporting component within the broader optimisation framework rather than as a standalone classifier. Its role is to provide indicative estimates that allow the subsequent filtering mechanism to exclude clearly unsafe actions. The tolerance parameter (τ) used in the filtering step increases the recall of acceptable actions to 0.81 for pedestrians and 0.96 for vehicles, which reduces the likelihood of overlooking unsafe outcomes. Given this arrangement, the current model performance is sufficient for guiding the multi-objective optimisation. A more detailed investigation of alternative prediction architectures and training strategies represents a valuable opportunity for future work.

Subsequently, the proposed MOMSATC workflow was implemented as a control policy within the simulator, intervening in the decision-making process by informing it of predicted performance outcomes. The following section details a scenario simulating arbitrary weekday rush hour demand, repeated with 20 different random seeds to ensure result reproducibility and mitigate potential bias arising from stochastic traffic arrival patterns. Reported results represent the mean cumulative performance and associated 95% confidence intervals.

Tables 5 and 6 present the origin-destination (OD) matrices for vehicles and pedestrians, respectively. Each OD matrix comprises four sub-matrices, each representing a 15-min interval. Each cell within a sub-matrix indicates the total demand travelling from the corresponding origin zone to the destination zone during that interval. The second, third and fourth quarter-hour matrices are scaled by factors of 1.1, 1.3 and 0.9, respectively, relative to the first quarter-hour matrix, simulating an hour of traffic demand variability. Subsequent performance evaluations will be based on the cumulative performance over 1 h.

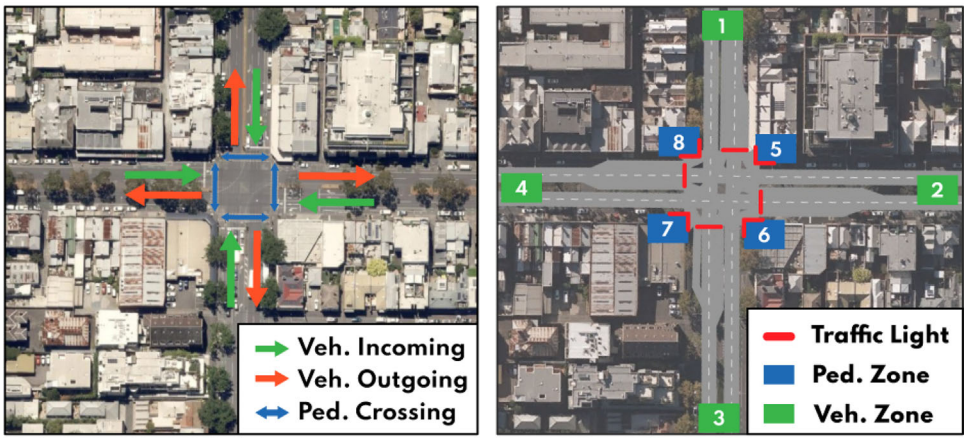

FIGURE 6 | Illustration of the four lane and four approach intersection within the AIMES testbed.

TABLE 5 | Vehicle OD matrices.

Period	O\D	1	2	3	4
00:00-15:00	**1**	0	50	100	30
	2	35	0	25	80
	3	100	50	0	20
	4	25	80	35	0
15:00-30:00	**1**	0	55	110	33
	2	39	0	28	88
	3	110	55	0	22
	4	28	88	39	0
30:00-45:00	**1**	0	65	130	39
	2	46	0	33	104
	3	130	65	0	26
	4	33	104	46	0
45:00-60:00	**1**	0	45	90	27
	2	32	0	23	72
	3	90	45	0	18
	4	23	72	32	0

TABLE 6 | Pedestrian OD matrices.

Period	O\D	5	6	7	8
00:00-15:00	**5**	0	40	0	40
	6	40	0	40	0
	7	0	40	0	40
	8	40	0	40	0
15:00-30:00	**5**	0	44	0	44
	6	44	0	44	0
	7	0	44	0	44
	8	44	0	44	0
30:00-45:00	**5**	0	52	0	52
	6	52	0	52	0
	7	0	52	0	52
	8	52	0	52	0
45:00-60:00	**5**	0	36	0	36
	6	36	0	36	0
	7	0	36	0	36
	8	36	0	36	0

Multiple methods have also been developed for benchmarking and comparison. The descriptions of each model are as follows:

1. MOMSATC: This is the proposed framework incorporating the MOMSTAC, as discussed in Section 3.4. In this model, both delay and safety are considered as optimisation objectives. Unlike DRL, which employs a black-box control policy to handle multiple objectives by assigning weights, MOMSTAC (a predictive analytics model) provides a more transparent structure for prioritising objectives. For example, the MOMSTAC in this study uses a filtering process that prioritises pedestrian safety. Any actions remaining for selection in subsequent steps must satisfy a predefined safety threshold.
2. Actuated: This model represents a standard actuated signal control system and reflects the most commonly implemented logic in real-world Australian intersections, particularly under the Sydney Coordinated Adaptive Traffic System [83, 84]. Similar systems, such as SCOOT [85], use field sensors including inductive loops and pedestrian push buttons to detect demand and adjust green time extensions based on observed traffic gaps. Given its widespread deployment and operational maturity, the actuated controller serves as the primary baseline for this study. All percentage improvements or deteriorations reported in the results are calculated relative to this model, allowing performance to be interpreted directly against current industry practice.
3. DDPG: This model adopts the deep deterministic policy gradient (DDPG) framework, a widely recognised DRL model for continuous control tasks [86], commonly applied in DRL traffic signal control research [87]. In this study, the DDPG model is trained to optimise delay rewards, illustrating the

FIGURE 7 | Comparison of the PMs throughout the testing period.

potential trade-offs between safety and efficiency in scenarios where the model focuses solely on efficiency objectives.

Consequently, Figure 7 compares the performance of the three control policies: MOMSATC (blue), actuated (orange) and DDPG (green), providing insight into the effectiveness of each model in optimising safety and efficiency objectives. The subplots in Figure 7 present the average cumulative performance measures (PMs) over the simulated hour (curves), along with their associated 95% confidence intervals (shaded areas). The performance measures considered are:

1. Cumulative safety cost for pedestrian–vehicle and vehicle–vehicle interactions, evaluated in dollars.

TABLE 7 | Averaged cumulative performance metrics result after 20 simulation sessions with 95% confidence interval.

	Actuated	MOMSATC	DDPG	Improvement %	
PM	**1**	**2**	**3**	**2 vs 1**	**3 vs 1**
Pedestrian safety cost ($)	8029 ± 6596	4300 ± 4339	9683 ± 4653	−46.4%	+20.6%
Vehicle safety cost ($)	8703 ± 8884	4526 ± 6515	69728 ± 110236	−47.9%	+700%
Pedestrian delays (s)	73939 ± 827	92957 ± 1733	65566 ± 2652	+25.7%	−11.3%
Vehicle delays (s)	77749 ± 728	85453 ± 2044	71699 ± 1668	+9.9%	−7.7%

2. Cumulative delay for pedestrians and vehicles, evaluated in user-seconds.

The subplots are arranged in descending order of optimisation priority in the MOMSTAC model's multiple-step optimisation process, with pedestrian safety as the primary objective and total user delays (pedestrians and vehicles) as the last objective. The horizontal axis represents time throughout the hourly simulation in seconds. Due to the MOMSATC model's 5-min observation period, its intervention activates after 300 s; before this, actions are randomly assigned. The MOMSATC intervention demonstrates efficacy after 500 s. Table 7 summarises the mean cumulative PMs and their associated 95% confidence intervals. The improvement column quantifies the percentage change of each PM relative to the baseline model (actuated).

The results demonstrate a significant improvement in pedestrian safety performance (−46.4%) when utilising the MOMSATC framework, along with notable enhancements in vehicle safety (−47.9%). These safety gains, however, come at the cost of increased delays for both pedestrians and vehicles, which rise by 25.7% and 9.9%, respectively. By contrast, the DDPG model reduces delays for pedestrians (−11.3%) and vehicles (−7.4%) but exhibits a substantial deterioration in safety performance, worsening pedestrian safety (+20.6%) and dramatically increasing vehicle conflict risk (+700%). This pattern suggests that optimisation focused primarily on delay reduction may inadvertently select actions that compromise safety.

This behaviour is consistent with findings from our earlier work on safe reinforcement learning for adaptive traffic control [60], which showed that combining multiple objectives into a single reward function can lead to unstable or unintended trade-offs. In that study, safety–efficiency interactions were encoded implicitly through reward weights, allowing delay-minimising actions to dominate even when they compromised safety. This empirical evidence informs the design rationale of the present framework.

In MOMSATC, safety improvements arise directly from its sequential optimisation architecture. In the first two stages, the cost-based safety evaluation assigns high monetary penalties to actions associated with low TTC values or high estimated crash severity, eliminating unsafe actions before any optimisation related to delay is undertaken. Because this filtering precedes delay minimisation, the remaining action set consists only of options that satisfy minimum safety requirements. This mechanism leads to the substantial reduction in pedestrian and vehicle conflict costs evident in the results. The accompanying increases in delay are a natural consequence of the restricted action space because once high-risk actions are eliminated, fewer timing strategies remain to efficiently serve traffic demand.

Overall, the findings underscore the inherent challenges in multi-objective optimisation, particularly when balancing competing objectives such as safety and delay. Although the degree of trade-off has been mitigated compared to prior work, it remains present. MOMSATC highlights the potential of parallel optimisation of safety and delay, offering a novel method for managing objectives with distinct units and magnitudes.

While the substantial improvement in pedestrian safety demonstrates the efficacy of the prioritisation strategy, diminishing returns observed in subsequent objectives underscore the inherent trade-offs within a sequential multi-objective optimisation framework. This outcome arises from the progressive reduction of the action space at each filtering stage, which may inadvertently exclude globally optimal solutions for subsequent objectives that fall outside the locally optimal subset. Additionally, the chosen tolerance value (τ), designed to minimise false negatives and ensure reliability in filtered actions, may inadvertently increase the likelihood of false positives. This conservative approach could lead to the premature exclusion of viable actions in later stages, thereby limiting further optimisation potential.

These observations suggest several avenues for future research. Enhancing the prediction model's accuracy in capturing extreme safety performance outcomes through refinement and the incorporation of more sophisticated machine learning techniques could improve overall efficacy. Furthermore, a systematic exploration of the impact of varying tolerance values (τ) and threshold values ($\alpha_{\eta,\,\mathrm{th}}$) on the optimisation process may yield valuable insights, facilitating a more balanced trade-off between safety and efficiency.

5 | Conclusion

This paper aims to promote active transport modes, a vital component of sustainable urban transport development, by addressing pedestrian safety at intersections from a traffic operations perspective. To achieve this, MOMSATC, a novel MOMSATC framework, is introduced, applying MPC principles to iteratively optimise traffic signals based on predicted outcomes. MOMSATC forecasts the impacts of feasible actions and selects the optimal action for implementation, enhancing safety and efficiency. A key contribution is the identification of two-phase signal programs that prioritise pedestrian safety. Additionally, a comprehensive hybrid safety evaluation framework was developed to support the

training and evaluation of the MTL model. This model predicts safety and delay outcomes by assessing both the likelihood and severity of conflicts involving VRU. The predicted safety cost metric serves as a key input for informed decision-making.

The MOMSATC framework's effectiveness was demonstrated in a case study conducted at an isolated intersection within the AIMES testbed. Results showed a substantial improvement in pedestrian safety, with a 46.4% reduction in safety costs compared to the baseline model, alongside notable improvements in vehicle safety (47.9% reduction). However, these gains in safety came with moderate increases in delays for both pedestrians and vehicles, highlighting the trade-offs inherent in a multi-objective optimisation framework. The study also revealed the challenges of balancing safety and efficiency, particularly the diminishing returns observed in optimising secondary objectives due to the sequential filtering process. This sequential approach, while effective in prioritising safety, may progressively restrict the action space, potentially excluding globally optimal solutions for subsequent objectives. Additionally, the conservative tolerance settings applied to enhance reliability could lead to the premature exclusion of viable actions in later stages.

Overall, the findings confirm that an interpretable, safety prioritised control structure can meaningfully enhance VRU protection while maintaining acceptable operational performance. The study also underscores the broader complexity of balancing competing objectives in adaptive traffic control and highlights the need for advanced approaches that manage interactions between safety and efficiency in a transparent and structured way.

Beyond the case study, the framework offers practical potential for real world deployment. As MOMSATC operates as a supervisory decision layer that evaluates feasible signal actions and identifies the safest and most efficient option, it can be integrated alongside existing signal control architectures without displacing established field logic. Its reliance on predicted safety and delay outcomes means that it can function with a range of sensing configurations, and its performance would further benefit from connected and automated vehicle environments where richer trajectory information is available. The computational demands of the optimisation process are modest, making real time implementation feasible on standard roadside processors or within centralised control centres. These characteristics position MOMSATC as a viable pathway towards deploying safety prioritised optimisation within operational traffic management systems.

5.1 | Future Work

This study focuses on establishing the feasibility and demonstrating the safety benefits of the MOMSATC framework within an MPC-based decision structure. Several extensions may further strengthen the framework and broaden its applicability.

Firstly, additional interpretability analyses could be undertaken to deepen understanding of the sequential filtering mechanism. Potential directions include visualising the evolution of feasible actions across optimisation stages and examining how decision boundaries shift under different objective priorities.

Secondly, broader benchmarking represents a valuable avenue for future research. Although this study evaluates MOMSATC against an actuated control baseline and a representative DRL model, incorporating additional multi objective MPC-based controllers or advanced learning based methods would provide a more comprehensive empirical context. In parallel, systematic ablation studies could help isolate the contributions of key components within the framework. Possible targets include the multi-step optimisation structure and the safety first filtering logic, each of which plays a distinct role in shaping the resulting control policies.

Finally, improving the prediction model remains an important direction. Enhancing its ability to capture extreme safety outcomes, together with systematic investigations into the effects of tolerance and threshold settings, may support a more balanced trade off between safety and efficiency. Further validation using real-world safety observations, such as empirical speed or conflict datasets, would strengthen the reliability of predicted safety costs and refine the sequential filtering mechanism. Extending the framework to multi-intersection or network level control, as well as adapting it to non Australian contexts through appropriate local calibration, also presents promising opportunities for further development.

Author Contributions

Lok Sang Chan: conceptualization, methodology, software, validation, visualization, writing – original draft, writing – review and editing. **Xiaocai Zhang:** conceptualization, methodology, software, supervision, writing – review and editing. **Neema NAssir:** funding acquisition, methodology, supervision, writing – review and editing. **Majid Sarvi:** funding acquisition, supervision, writing – review and editing.

Acknowledgements

This research was funded by ARC LP200301389, Kapsch TrafficCom Australia, RACQ, and iMOVE CRC, the Cooperative Research Centres program, an Australian Government initiative.

Conflicts of Interest

The authors declare no conflicts of interest.

Data Availability Statement

The data that support the findings of this study are available from the corresponding author upon reasonable request.

References

1. G. Broadbent, C. Allen, T. Wiedmann, and G. Metternicht, "The Role of Electric Vehicles in Decarbonising Australia's Road Transport Sector: Modelling Ambitious Scenarios," *Energy Policy* 168 (2022): 113144, https://doi.org/10.1016/j.enpol.2022.113144.

2. T. Batool, V. Ross, J. Blerk, et al., "Promoting Sustainable Transportation: A Transtheoretical Examination of Active Transport Modes," *Sustainability (Switzerland)* 16 (2024): 472, https://doi.org/10.3390/su16020472.

3. B. Liao, P. E. W. van den Berg, P. J. V. van Wesemael, and T. A. Arentze, "Empirical Analysis of Walkability Using Data From the Netherlands," *Transportation Research: Part D: Transport and Environment* 85 (2020): 102390.

4. V. Kunaratnam, N. Schwartz, A. Howard, et al., "Equity, Walkability, and Active School Transportation in Toronto, Canada: A Cross-Sectional Study," *Transportation Research Part D* 108 (2022): 103336, https://doi.org/10.1016/j.trd.2022.103336.

5. World Health Organization, *Global Status Report on Road Safety 2023* (World Health Organization, 2023).

6. Bureau of Infrastructure and Transport Research Economics, *Road Trauma Australia 2022 Statistical Summary* (BITRE, Canberra ACT, 2023).

7. M. Nasri, K. Aghabayk, A. Esmaili, and N. Shiwakoti, "Using Ordered and Unordered Logistic Regressions to Investigate Risk Factors Associated With Pedestrian Crash Injury Severity in Victoria, Australia," *Journal of Safety Research* 81 (2022): 78–90, https://doi.org/10.1016/j.jsr.2022.01.008.

8. P. Chen, W. Zeng, G. Yu, and Y. Wang, "Surrogate Safety Analysis of Pedestrian-Vehicle Conflict at Intersections Using Unmanned Aerial Vehicle Videos," *Journal of Advanced Transportation* 2017 (2017): 5202150, https://doi.org/10.1155/2017/5202150.

9. B. Lv, R. Sun, H. Zhang, H. Xu, and R. Yue, "Automatic Vehicle-Pedestrian Conflict Identification With Trajectories of Road Users Extracted From Roadside LiDAR Sensors Using a Rule-Based Method," *IEEE Access: Practical Innovations, Open Solutions* 7 (2019): 161594–161606, https://doi.org/10.1109/ACCESS.2019.2951763.

10. J. Wu, H. Xu, Y. Zhang, and R. Sun, "An Improved Vehicle-Pedestrian Near-Crash Identification Method With a Roadside LiDAR Sensor," *Journal of Safety Research* 73 (2020): 211–224, https://doi.org/10.1016/j.jsr.2020.03.006.

11. S. Zhang, M. Abdel-Aty, Q. Cai, P. Li, and J. Ugan, "Prediction of Pedestrian-Vehicle Conflicts at Signalized Intersections Based on Long Short-Term Memory Neural Network," *Accident Analysis & Prevention* 148 (2020): 105799, https://doi.org/10.1016/j.aap.2020.105799.

12. S. Zhang and M. Abdel-Aty, "Real-Time Pedestrian Conflict Prediction Model at the Signal Cycle Level Using Machine Learning Models," *IEEE Open Journal of Intelligent Transportation Systems* 3 (2022): 176–186, https://doi.org/10.1109/OJITS.2022.3155126.

13. N. Anwari, M. Abdel-Aty, A. Goswamy, and O. Zheng, "Investigating Surrogate Safety Measures at Midblock Pedestrian Crossings Using Multivariate Models With Roadside Camera Data," *Accident Analysis & Prevention* 192 (2023): 107233.

14. S. Singh, Y. Ali, and M. M. Haque, "A Bayesian Extreme Value Theory Modelling Framework to Assess Corridor-Wide Pedestrian Safety Using Autonomous Vehicle Sensor Data," *Accident Analysis & Prevention* 195 (2024): 107416, https://doi.org/10.1016/j.aap.2023.107416.

15. F. Hussain, Y. Ali, Y. Li, and M. M. Haque, "Revisiting the Hybrid Approach of Anomaly Detection and Extreme Value Theory for Estimating Pedestrian Crashes Using Traffic Conflicts Obtained From Artificial Intelligence-Based Video Analytics," *Accident Analysis & Prevention* 199 (2024): 107517, https://doi.org/10.1016/j.aap.2024.107517.

16. J. Archer, N. Fotheringham, M. Symmons, and B. Corben, *The Impact of Lowered Speed Limits in Urban/Metropolitan Areas*, Report No. 276 (Monash University Accident Research Centre, 2008).

17. G. Andersson and G. Nilsson, *Speed Management in Sweden: Speed, Speed Limits and Safety* (Swedish National Road and Transport Research Institute, 1997).

18. N. Lubbe, Y. Wu, and H. Jeppsson, "Safe Speeds: Fatality and Injury Risks of Pedestrians, Cyclists, Motorcyclists, and Car Drivers Impacting the Front of Another Passenger Car as a Function of Closing Speed and Age," *Traffic Safety Research* 2 (2022): 000006.

19. Y. Ni, M. Wang, J. Sun, and K. Li, "Evaluation of Pedestrian Safety at Intersections: A Theoretical Framework Based on Pedestrian-Vehicle Interaction Patterns," *Accident Analysis & Prevention* 96 (2016): 118–129, https://doi.org/10.1016/j.aap.2016.07.030.

20. Z. Ma, G. Mei, and S. Cuomo, "An Analytic Framework Using Deep Learning for Prediction of Traffic Accident Injury Severity Based on Contributing Factors," *Accident Analysis and Prevention* 160 (2021): 106322, https://doi.org/10.1016/j.aap.2021.106322.

21. Z. Sun, Y. Xing, J. Wang, X. Gu, H. Lu, and Y. Chen, "Exploring Injury Severity of Vulnerable Road User Involved Crashes Across Seasons: A Hybrid Method Integrating Random Parameter Logit Model and Bayesian Network," *Safety Science* 150 (2022): 105682, https://doi.org/10.1016/j.ssci.2022.105682.

22. A. Goswamy, M. Abdel-Aty, and Z. Islam, "Factors Affecting Injury Severity at Pedestrian Crossing Locations With Rectangular RAPID Flashing Beacons (RRFB) Using XGBoost and Random Parameters Discrete Outcome Models," *Accident Analysis and Prevention* 181 (2023): 106937, https://doi.org/10.1016/j.aap.2022.106929.

23. Z. Sun, D. Wang, X. Gu, et al., "A Hybrid Approach of Random Forest and Random Parameters Logit Model of Injury Severity Modeling of Vulnerable Road Users Involved Crashes," *Accident Analysis & Prevention* 192 (2023): 107235.

24. S. Lundberg and S.-I. Lee, "A Unified Approach to Interpreting Model Predictions," preprint, arXiv, May 22, 2017, https://arxiv.org/abs/1705.07874.

25. H. Al-Salman and R. Salter, "Control of Right-Turning Vehicles at Signal-Controlled Intersections," *Traffic Engineering and Control* 15, no. 15 (1974): 683–686.

26. R. Goldblatt, F. Mier, and J. Friedman, "Continuous Flow Intersections," *ITE Journal* 64 (1994): 35–35.

27. M. Alzoubaidi and M. Zlatkovic, "Operational Assessment of Continuous Flow Intersections in a Connected Vehicle Environment," *Transportation Planning and Technology* 45, no. 6 (2022): 524–543.

28. Y. Xuan, C. F. Daganzo, and M. J. Cassidy, "Increasing the Capacity of Signalized Intersections With Separate Left Turn Phases," *Transportation Research Part B: Methodological* 45, no. 5 (2011): 769–781, https://doi.org/10.1016/j.trb.2011.02.009.

29. C. Yan, H. Jiang, and S. Xie, "Capacity Optimization of an Isolated Intersection Under the Phase Swap Sorting Strategy," *Transportation Research Part B: Methodological* 60 (2014): 85–106, https://doi.org/10.1016/j.trb.2013.12.001.

30. P. Kozey, Y. Xuan, and M. J. Cassidy, "A Low-Cost Alternative for Higher Capacities at Four-Way Signalized Intersections," *Transportation Research Part C: Emerging Technologies* 72 (2016): 157–167, https://doi.org/10.1016/j.trc.2016.09.012.

31. J. Murakami, C. Villani, and G. Talamini, "The Capital Value of Pedestrianization in Asia's Commercial Cityscape: Evidence From Office Towers and Retail Streets," *Transport Policy* 107 (2021): 72–86, https://doi.org/10.1016/j.tranpol.2021.04.017.

32. J. Cui, A. Allan, and D. Lin, "The Development of Grade Separation Pedestrian System: A Review," *Tunnelling and Underground Space Technology* 38 (2013): 151–160, https://doi.org/10.1016/j.aap.2021.106322.

33. R. Jagannathan and J. G. Bared, "Design and Performance Analysis of Pedestrian Crossing Facilities for Continuous Flow Intersections," *Transportation Research Record* 1939, no. 1 (2005): 133–144.

34. L. Leden, P. Gårder, and C. Johansson, "Safe Pedestrian Crossings for Children and Elderly," *Accident Analysis & Prevention* 38, no. 2 (2006): 289–294, https://doi.org/10.1016/j.aap.2005.09.012.

35. L. Li, X. Yang, and L. Yin, "Exploration of Pedestrian Refuge Effect on Safety Crossing at Signalized Intersection," *Transportation Research Record* 2193, no. 1 (2010): 44–50.

36. T. Wang, J. Zhao, C. Li, et al., "Pedestrian Delay Model for Continuous Flow Intersections Under Three Design Patterns," *Mathematical Problems in Engineering* 2019 (2019): 1016261.

37. L. Tang, Y. Liu, J. Li, et al., "Pedestrian Crossing Design and Analysis for Symmetric Intersections: Efficiency and Safety," *Transportation*

Research Part A: Policy and Practice 142 (2020): 187–206, https://doi.org/10.1016/j.tra.2020.10.012.

38. W. Ma, Y. Liu, and K. L. Head, "Optimization of Pedestrian Phase Patterns at Signalized Intersections: A Multi-Objective Approach," *Journal of Advanced Transportation* 48, no. 8 (2014): 1138–1152, https://doi.org/10.1002/atr.1256.

39. L. Chen, C. Chen, and R. Ewing, "Left-Turn Phase: Permissive, Protected, or Both? A Quasi-Experimental Design in New York City," *Accident Analysis & Prevention* 76 (2015): 102–109, https://doi.org/10.1016/j.aap.2014.12.019.

40. T. Urbanik, A. Tanaka, B. Lozner, et al., *Signal Timing Manual* (Transportation Research Board, 2015).

41. C. M. Abrams and S. A. Smith, "Selection of Pedestrian Signal Phasing," *Transportation Research Record* 629 (1977): 1–6.

42. C. V. Zegeer, K. S. Opiela, and M. J. Cynecki, "Effect of Pedestrian Signals and Signal Timing on Pedestrian Accidents," *Transportation Research Record: Journal of the Transportation Research Board* 847 (1982): 62–72.

43. D. M. Zaidel and I. Hocherman, "Safety of Pedestrian Crossings at Signalized Intersections," *Transportation Research Record* 1141 (1987): 1–6.

44. P. Gårder, "Pedestrian Safety at Traffic Signals: A Study Carried Out With the Help of a Traffic Conflicts Technique," *Accident Analysis & Prevention* 21, no. 5 (1989): 435–444.

45. A. K. Bechtel, K. E. MacLeod, and D. R. Ragland, "Pedestrian Scramble Signal in Chinatown Neighborhood of Oakland, California: An Evaluation," *Transportation Research Record* 1878, no. 1 (2004): 19–26, https://doi.org/10.3141/1878-03.

46. L. Kattan, S. Acharjee, and R. Tay, "Pedestrian Scramble Operations: Pilot Study in Calgary, Alberta, Canada," *Transportation Research Record* 2140, no. 1 (2009): 79–84, https://doi.org/10.3141/2140-08.

47. Y. Zhang, S. A. Mamun, J. N. Ivan, N. Ravishanker, and K. Haque, "Safety Effects of Exclusive and Concurrent Signal Phasing for Pedestrian Crossing," *Accident Analysis & Prevention* 83 (2015): 26–36, https://doi.org/10.1016/j.aap.2015.06.010.

48. J. N. Ivan, K. McKernan, Y. Zhang, N. Ravishanker, and S. A. Mamun, "A Study of Pedestrian Compliance With Traffic Signals for Exclusive and Concurrent Phasing," *Accident Analysis & Prevention* 98 (2017): 157–166, https://doi.org/10.1016/j.aap.2016.10.003.

49. A. Arun, C. Lyon, T. Sayed, et al., "Leading Pedestrian Intervals – Yay or Nay? A Before-After Evaluation of Multiple Conflict Types Using an Enhanced Non-Stationary Framework Integrating Quantile Regression Into Bayesian Hierarchical Extreme Value Analysis," *Accident Analysis & Prevention* 181 (2023): 106929, https://doi.org/10.1016/j.aap.2022.106929.

50. W. Du, J. Ye, J. Gu, J. Li, H. Wei, and G. Wang, "Safelight: A Reinforcement Learning Method Toward Collision-Free Traffic Signal Control," *Proceedings of the AAAI Conference on Artificial Intelligence* 37 (2022): 14801–14810.

51. X. Li and J.-Q. Sun, "Intersection Multi-Objective Optimization On Signal Setting and Lane Assignment," *Physica A: Statistical Mechanics and its Applications* 525 (2019): 1233–1246, https://doi.org/10.1016/j.physa.2019.04.223.

52. A. Stevanovic, J. Stevanovic, J. So, and M. Ostojic, "Multi-Criteria Optimization of Traffic Signals: Mobility, Safety, and Environment," *Engineering and Applied Sciences Optimization (OPT-i) - Professor Matthew G. Karlaftis Memorial Issue* 55 (2015): 46–68.

53. Y. Gong, M. Abdel-Aty, J. Yuan, and Q. Cai, "Multi-Objective Reinforcement Learning Approach for Improving Safety at Intersections With Adaptive Traffic Signal Control," *Accident Analysis & Prevention* 144 (2020): 105655, https://doi.org/10.1016/j.aap.2020.105655.

54. K. Xu, J. Huang, L. Kong, J. Yu, and G. Chen, "PV-TSC: Learning to Control Traffic Signals for Pedestrian and Vehicle Traffic in 6G Era," *IEEE Transactions on Intelligent Transportation Systems* 24, no. 7 (2022): 7552–7563.

55. M. Yazdani, M. Sarvi, S. Asadi Bagloee, N. Nassir, J. Price, and H. Parineh, "Intelligent Vehicle Pedestrian Light (IVPL): A Deep Reinforcement Learning Approach For Traffic Signal Control," *Transportation Research Part C: Emerging Technologies* 149 (2023): 103991, https://doi.org/10.1016/j.trc.2022.103991.

56. G. Zhang, F. Chang, J. Jin, F. Yang, and H. Huang, "Multi-Objective Deep Reinforcement Learning Approach for Adaptive Traffic Signal Control System With Concurrent Optimization of Safety, Efficiency, and Decarbonization at Intersections," *Accident Analysis & Prevention* 199 (2024): 107451.

57. H. Jiang, Z. Yao, Y. Zhang, Y. Jiang, and Z. He, "Pedestrian Shuttle Service Optimization for Autonomous Intersection Management," *Transportation Research Part C: Emerging Technologies* 163 (2024): 104623.

58. G. Zhang, H. Huang, and F. Chang, "TS-PVL: Two-Stage Deep Reinforcement Learning-Based Traffic Light With Pedestrian-Vehicle Control in Mixed-Autonomy Traffic," *IEEE Internet of Things Journal* 12, no. 15 (2025): 31001–31014.

59. A. D. Ren, B. G. Zhang, C. F. Chang, and D. H. Huang, "Two-Step Deep Reinforcement Learning for Traffic Signal Control to Improve Pedestrian Safety Using Connected Vehicle Data," *Accident Analysis & Prevention* 222 (2025): 108161.

60. L. S. Chan, N. Nassir, X. Zhang, M. Yazdani, and M. Sarvi, "Preemptive Crash Risk Reduction Through a Real-Time Cost-Based Safety Prediction Model (RECOSAM) for Traffic Signal Control," *Computers and Electrical Engineering* 128 (2025): 110639.

61. Transport Accident Commision, *TAC Road Safety Quarterly Statistics Report* (TAC, 2023).

62. F. Hussain, Y. Li, A. Arun, and M. M. Haque, "A Hybrid Modelling Framework of Machine Learning and Extreme Value Theory for Crash Risk Estimation Using Traffic Conflicts," *Analytic Methods in Accident Research* 36 (2022): 100248, https://doi.org/10.1016/j.amar.2022.100248.

63. C. Oh and T. Kim, "Estimation of Rear-End Crash Potential Using Vehicle Trajectory Data," *Accident Analysis and Prevention* 42, no. 6 (2010): 1888–1893, https://doi.org/10.1016/j.aap.2010.05.009.

64. L. N. Peesapati, M. P. Hunter, and M. O. Rodgers, "Evaluation of Postencroachment Time as Surrogate for Opposing Left-Turn Crashes," *Transportation Research Record* 2386, no. 1 (2013): 42–51.

65. A. P. Tarko, "A Unifying View On Traffic Conflicts and Their Connection With Crashes," *Accident Analysis & Prevention* 158 (2021): 106187, https://doi.org/10.1016/j.aap.2021.106187.

66. L. Zheng, T. Sayed, and F. Mannering, "Modeling Traffic Conflicts for Use in Road Safety Analysis: A Review of Analytic Methods and Future Directions," *Analytic Methods in Accident Research* 29 (2021): 100142, https://doi.org/10.1016/j.amar.2020.100142.

67. L. Zheng and T. Sayed, "A Bivariate Bayesian Hierarchical Extreme Value Model for Traffic Conflict-Based Crash Estimation," *Analytic Methods in Accident Research* 25 (2020): 100111.

68. D. A. Hensher, "Value of Life and Injuries," in *International Encyclopedia of Transportation*, ed. R. Vickerman (Elsevier, 2021), 737–741, https://doi.org/10.1016/B978-0-08-102671-7.10205-2.

69. D. A. Hensher, J. M. Rose, J. D. D. Ortúzar, and L. I. Rizzi, "Estimating the Willingness to Pay and Value of Risk Reduction for Car Occupants in the Road Environment," *Transportation Research Part A* 43, no. 7 (2009): 692–707, https://doi.org/10.1016/j.tra.2009.06.001.

70. R.-C. Jou, D. A. Hensher, T.-Y. Chen, and M.-C. Chao, "Hospitalisation Costs and Duration of Elderly Motorcyclists' Non-Fatality Crashes in Taiwan," *International Journal of Injury Control and Safety Promotion* 20, no. 2 (2013): 158–168, https://doi.org/10.1016/j.enpol.2022.113144.

71. Transport for New South Wales, *Transport for NSW Economic Parameter Values*, TfNSW Technical Report (Transport for New South Wales, 2020).

72. PTV Group (PTV Planung Transport Verkehr), *PTV Vissim 2022 User Manual* (PTV AG, 2022), 1352.

73. Federal Highway Administration (FHWA), *Surrogate Safety Assessment Model, 2017 Enhancement and Update: SSAM Version 3.0*, FHWA-HRT-17-027 (Federal Highway Administration, January 2017).

74. Y. Guo, T. Sayed, L. Zheng, and M. Essa, "An Extreme Value Theory Based Approach for Calibration of Microsimulation Models for Safety Analysis," *Simulation Modelling Practice and Theory* 106 (2021): 102172, https://doi.org/10.1016/j.simpat.2020.102172.

75. Y. Guo, M. Essa, T. Sayed, M. M. Haque, and S. Washington, "A Comparison Between Simulated and Field-Measured Conflicts for Safety Assessment of Signalized Intersections in Australia," *Transportation Research Part C* 101 (2019): 96–110.

76. C. Katrakazas, M. Quddus, and W.-H. Chen, "A Simulation Study of Predicting Real-Time Conflict-Prone Traffic Conditions," *IEEE Transactions on Intelligent Transportation Systems* 19, no. 10 (2017): 3196–3207.

77. U. Shahdah, F. Saccomanno, and B. Persaud, "Application of Traffic Microsimulation for Evaluating Safety Performance of Urban Signalized Intersections," *Transportation Research Part C* 60 (2015): 96–104.

78. J. C. Hayward, *Near Miss Determination through Use of a Scale of Danger* (Pennsylvania Transportation and Traffic Safety Center, 1972).

79. P. J. Cooper, "Experience With Traffic Conflicts in Canada With Emphasis on 'Post Encroachment Time' Techniques," in *International Calibration Study of Traffic Conflict Techniques*, ed. E. Asmussen (Springer, 1984), 75–96, https://doi.org/10.1007/978-3-642-82109-7_8.

80. S. M. S. Mahmud, L. Ferreira, M. S. Hoque, and A. Tavassoli, "Micro-Simulation Modelling for Traffic Safety: A Review and Potential Application to Heterogeneous Traffic Environment," *IATSS Research* 43, no. 1 (2019): 27–36, https://doi.org/10.1016/j.iatssr.2018.07.002.

81. C. Johnsson, A. Laureshyn, and C. Dágostino, "A Relative Approach to the Validation of Surrogate Measures of Safety," *Accident Analysis & Prevention* 161 (2021): 106350, https://doi.org/10.1016/j.aap.2021.106350.

82. B.-L. Ye, W. Wu, K. Ruan, L. Li, T. Chen, H. Gao, and Y. Chen, "A Survey of Model Predictive Control Methods for Traffic Signal Control," *IEEE/CAA Journal of Automatica Sinica* 6, no. 3 (2019): 623–640.

83. A. G. Sims, "The Sydney Coordinated Adaptive Traffic System," in *Engineering Foundation Conference on Research Directions in Computer Control of Urban Traffic Systems* (Pacific Grove, 1979), 12–27.

84. A. G. Sims and K. W. Dobinson, "The Sydney Coordinated Adaptive Traffic (SCAT) System Philosophy and Benefits," *IEEE Transactions on Vehicular Technology* 29, no. 2 (1980): 130–137.

85. P. B. Hunt, D. I. Robertson, R. D. Bretherton, and R. I. Winton, *SCOOT-a Traffic Responsive Method of Coordinating Signals*, TRRL Laboratory Report1014 (Transport and Road Research Laboratory, 1981).

86. T. P. Lillicrap, "Continuous Control With Deep Reinforcement Learning," preprint, arXiv, September 9, 2015, https://arxiv.org/abs/1509.02971.

87. N. Casas, "Deep Deterministic Policy Gradient for Urban Traffic Light Control," preprint, arXiv, March 24, 2017, https://arxiv.org/abs/1703.09035.